

BASIC INVESTIGATION ON CORROSION DETECTION OF PRESTRESSING STEEL BARS BASED ON MAGNETIC FLUX LEAKAGE METHOD

Artur SAGRADYAN*¹, Satoshi TAKAYA*² and Takashi YAMAMOTO*³

ABSTRACT

The paper presents the methodology for detection of corrosion damage of prestressing steel bars in post-tensioned prestressed concrete structures. The proposed methodology pertains to non-destructive testing methods based on magnetic flux leakage. The results demonstrated that the methodology allows to detect loss of cross-section of prestressing steel bars due to corrosion, establish location of the damaged site and approximately evaluate its degree. The results of the experiments conform to the results of simulation carried out using Finite Element Method.

Keywords: Magnetic flux leakage, prestressing steel bar, corrosion, NDT, FEM analysis.

1. INTRODUCTION

Corrosion of prestressing steel bars embedded in prestressed concrete (hereinafter, PC) structures is a well-known dangerous phenomenon; in particular, it can lead to rupture of prestressing steel bars. Therefore timely prediction and evaluation of prestressing steel bars' corrosion is a topical issue in a field of civil engineering infrastructure. Currently used methods for its detection are, mainly, electrochemical methods. They are extensively studied and widely applied, but at the same time they possess some limitations. In particular, it is difficult to obtain information about degree of corrosion in terms of a decrease of a cross-section or a weight-loss by means of electrochemical methods. They are also influenced by temperature, humidity and quality of electric contact with reinforcement bars [1]. Moreover, in a case of prestressing steel bars in PC, sheaths make electrochemical results complicated. Therefore, alternative non-destructive testing (NDT) methods for detection of prestressing steel bars' corrosion are required.

In that regard, a magnetic flux leakage (MFL) method seems useful. The method is successfully used in many industries, related with quality control and inspection of steel products, including detection of corrosion-related damage [2, 3]. Also the method is reported to be effective in detection of rupture of reinforcing steel bars of concrete structures [4-8]. One of the strong points of MFL method in a case of its application in concrete is the fact, that magnetic permeability of regular concrete is almost the same as magnetic permeability of air. Therefore, concrete itself, generally, has no influence on results of testing. Also, MFL method is, generally, not influenced by temperature and humidity. Moreover, in a case of prestressing steel bars in PC structures, the authors presume that sheath has a minor influence on results of

MFL testing of prestressing steel bars. That opinion is supported by results of experiment, which is presented in the chapter 3.1.

The MFL method, mainly, consists of magnetization of the targeted magnetic object (e.g., prestressing steel bar) and scanning of it with sensors of a certain type. Cross sectional loss caused by corrosion or mechanical damage leads to change of MFL density. That change can be detected by sensors, thus, allowing detection of a defect and evaluation of its degree.

Very few studies have been performed regarding corrosion detection of PC bars by means of MFL devices [4, 7], while that method can offer advantages, which seem beneficial for NDT testing of PC structures. The presented study is focused on the development of new methodology of corrosion detection of PC bars by means of MFL method.

2. METHODOLOGY

2.1 Background of the study and the proposed methodology of MFL testing

The device used for experiments in the presented study is introduced in detail in the study of Makoto Hirose et al. [8]. It consists of a permanent magnet and a scanning unit with two coil-type sensors. The device is light-weight and doesn't require supply of electricity.

That device was initially designed for detection of ruptures of reinforcement. For that reason the methodology proposed by the producer is not sensitive enough to detect damage done by corrosion. In order to overcome that disadvantage, the new methodology was proposed and reported at JCI symposium in 2015 [9].

Basically, the proposed methodology consisted of division of the tested PC bar in several sectors, each of which was scanned separately. The results allowed to distinguish between the non-corroded and corroded steel bars with weight loss of, approximately, 5.5-8.6%.

However, the proposed methodology still

*1 Department of Civil & Earth Resources Engineering, Kyoto University, JCI Student Member

*2 Department of Civil & Earth Resources Engineering, Kyoto University, Assistant Professor, JCI Member

*3 Department of Civil & Earth Resources Engineering, Kyoto University, Associate Professor, JCI Member

required comparison with a non-corroded steel bar to make conclusions about the presence of corrosion PC bar. Also, the proposed conclusions were based on experimental results and lacked analytical justification.

The presented study has the aim to solve the aforementioned problems, as well as to clarify other important points in application of MFL method for corrosion detection of PC bars in concrete.

The methodology of MFL testing proposed in the presented study is an improved version of the methodology proposed in previous study [9]. The new point is scanning not only in forward, but also in backward direction. Presumably, it can allow to avoid use of a non-corroded specimen as a reference. Basically, it is related with decrease of MFL density, which takes place near a corroded zone of a steel bar; as the result, scanning in forward and backward direction will produce different results due to the change of position of zone with decreased MFL density relatively to the direction of scanning. That point is discussed in details in the section 3.1 of the presented paper.

The flowchart of the proposed methodology is presented in the Figure 1. The procedure begins with establishing of the scanned line, which is a projection of a tested PC bar on a surface of a tested structure; after that the scanned line is divided into several scanned sectors, which are consequently magnetized and scanned, firstly, in forward direction, and, after that, in the opposite direction.

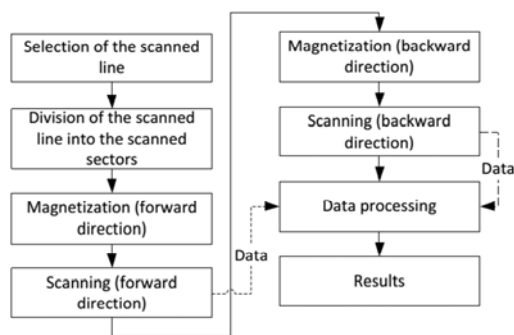


Fig. 1 Flowchart of the proposed methodology.

The obtained data is in a form of graphs position-MFL density for each of the scanned sectors in forward direction and for each of the scanned sectors in backward direction.

It is known that, with other conditions being equal, objects of lighter weight have lesser MFL density than heavier object. Therefore, considering that corrosion will lead to decrease of weight of PC bar, corroded parts of PC bar will be lighter than non-corroded, and, thus, MFL density of corroded parts will be lower than MFL density of non-corroded parts. Therefore, if a scanned sector of a tested PC bar corresponds to a corroded part of PC bar, its MFL density will be lower than MFL density of a scanned sector, which corresponds to a not damaged part of a PC bar.

In order to evaluate MFL density of a scanned sector, an area confined by a curve of position-MFL

density graph (hereinafter – S parameter) is calculated. S parameter value is calculated by means of method of trapezoids.

Thus, final results of the testing according to the proposed methodology are represented in a form of a graph, which vertical axis is a value of S parameter, and horizontal axes represent number of a scanned sector.

Identification of the damaged zones from the results of scanning in forward and backward directions can be carried out as follows. In the case a tested steel bar is not damaged, the results for scanning in forward and backward directions will be similar. However, in the case of a damaged steel bar the results for scanning in forward and backward direction will be different. Generally, significant difference between value of S parameter for scanning in forward direction for a given sector and value of S parameter for scanning in backward direction can be considered an indication of damage in that sector.

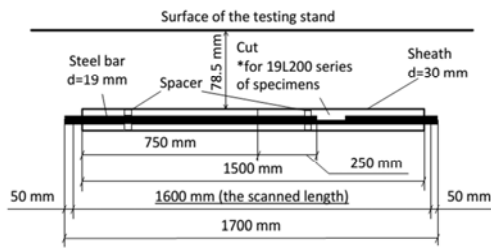
2.2 Experimental study

Experimental study was carried out in order to evaluate capability of the proposed methodology to detect damage to PC bar using simplified specimens simulating PC structural element. The specimens were steel sheath of $d=30$ mm (wall thickness – 0.7 mm) with PC bars of $d=19$ mm inside; PC bars were centered and fixed inside sheath by means of plastic spacers without grouting.

In order to simulate different levels of corrosion damage, artificial cuts of different length in longitudinal direction and depth were made on the steel bars. Cuts can be used to approximately simulate corrosion damage for following reasons. First, by making cut it is possible to achieve a certain decrease of cross-section accompanied by loss of weight, which is similar to effect of corrosion. However, in a case of corrosion, a certain type of corrosion products is formed, which depends on corrosion conditions. Generally, corrosion of PC bars is initiated by chloride ion, which ingress can be caused by sea water or de-icing salts. As it was demonstrated in the study of Takaya et al. [11], corrosion products that are formed during corrosion in a presence of chloride ion are mainly β -FeOOH and γ -FeOOH. However, they don't possess magnetic properties according to the data from literature [12], and, therefore, they don't have any influence on MFL density.

Experiment setup and specimens' parameters are summarized in Table 1 and Figure 2. The tested specimens were divided into 5 scanned sectors of the same length with the same shift. The layout of sectors is presented in Figure 3.

Not damaged reference specimen 19N was prepared for comparison and in order to establish difference between damaged and not damaged specimen. Also, specimen 19B, which is a steel bar of 19 mm diameter without sheath, was tested in order to estimate influence of sheath on the experiment result. The experiment setup for specimen 19B is similar to other specimens (see Figure 2).



*for 19L850 series of specimens half of bar was cut.
Fig. 2 Scheme of experiment setup.

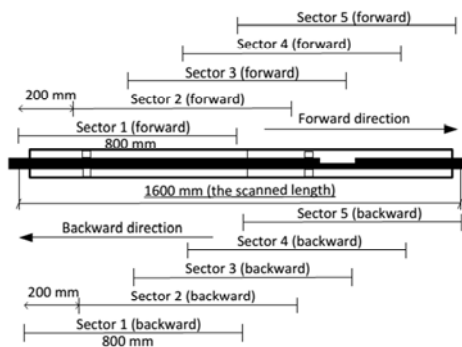


Fig. 3 Layout of the scanned sectors.

Table 1 Experiment setup

Specimen code	Cut length, mm	Cut depth, mm / % of cross section area decrease	Weight loss, g / g/cm ²
19B	n/a	n/a	n/a
19N (ref.)	n/a	n/a	n/a
19L200D1	200	1/2	18.89/0.04
19L200D2	200	2/6	38.07/ 0.08
19L200D3	200	3/10	51.23/ 0.1
19L200D4	200	4/15	75.85/ 0.15
19L850D1	850	1/2	65.38/ 0.13
19L850D2	850	2/6	148.05/ 0.29
19L850D3	850	3/10	237.68/ 0.47
19L850D4	850	4/15	318.26/ 0.63

All tests were carried out using the wooden testing stand; the design of the testing stand allows to freely place PC bars, stirrups and additional reinforcement in various combinations.

2.3 Analytical investigation

In order to provide analytical justification of the proposed methodology a numerical simulation was carried out in Finite Element Method on Magnetics (FEMM), which is a freeware suite of programs for solving low frequency electromagnetic problems on two-dimensional planar and axisymmetric domains [10]. The used MFL simulation software doesn't allow to carry out three-dimensional simulations and, therefore, correctly simulate influence of sheath (which is, in fact, is a hollow cylinder with thin walls), as well as to simulate redistribution of MFL density in the tested PC bar due to movement of the permanent magnet during the magnetization. Without taking into account those

factors, it is impossible to carry out accurate simulation; however, FEMM can be used for justification of basic points and relationships of the proposed methodology.

Thus, the aim of the analysis is only to prove main points of the proposed methodology, such as relationship between weight-loss and MFL and changes of MFL for scanning in opposite directions.

2.4 Parameters and procedure of the analysis

The analyzed object is a longitudinal cross-section of the PC bar of $d=19$ mm and length of 1700 mm. The material of the simulated PC bar was steel 1020; steel 1020 is included in material library of FEMM and its magnetic properties are specified by non-linear B-H curve, maximum hysteresis angle, electrical conductivity and coercivity of the material. The simulation domain is represented by a circle around the analyzed object, which is specified as air. Magnetization was simulated by means of setting up a certain value of coercivity to the PC bar.

Three cases were simulated: not damaged steel bar and steel bars with cuts of depth of 4 mm and lengths of 200 mm and 850 mm.

The procedure of analysis can be summarized as follows. The first stage is creation of geometry of the analyzed object. As the result, blocks of the analyzed objects are created (in the discussed case there is the block of the steel bar and the block of surrounding air). The next step is identification of material properties of the created blocks (in the discussed case it is air for the air block and steel 1020 for the steel bar). The next step is specification of boundary conditions (in the discussed case asymptotic boundary conditions are used, which are simulating an unbounded domain). The following stages include mesh generation, simulation and extraction of results.

3. RESULTS AND DISCUSSION

3.1 Results of the analysis

The results of the simulation are presented in Figure 4.

As it can be seen from the figure, MFL density at the part of a PC bar with the cut is significantly lower than for the not damaged part. It is related with a decrease of cross-section (and, thus, weight) caused by cutting. Moreover, decrease of MFL density is proportional to length of cut and, therefore, weight-loss. Thus, it proves that MFL density is influenced by decrease of cross-section or weight-loss, caused by corrosion or other effects.

Another conclusion is that in a case of scanning of the not damaged steel bar MFL density map is uniform. In the case of a steel bar presented in Figure 4a (not damaged steel bar), the scanning in forward direction (from left to right) will give the same results as the scanning in forward direction (from right to left) because both left and right sides are not damaged and, therefore, MFL density of left and right sides will be the same. However, in a case of a damaged steel bar, MFL density decreases at a place of a defect, and the

results for scanning in forward direction and backward direction will be different. For example, in the case of a steel bar presented in Figure 4c, scanning in forward direction (from left to right) will result in decrease of MFL density from the beginning of the steel bar (left, not damaged part, higher values of MFL density) to the end of the steel bar (right, damaged part, lower values of MFL density), and the scanning in backward direction (from right to left) will result in the increase of S parameter from the end of the steel part (right, damaged part, lower values of MFL density) to the beginning of the steel bar (left, not damaged part, higher values of MFL density).

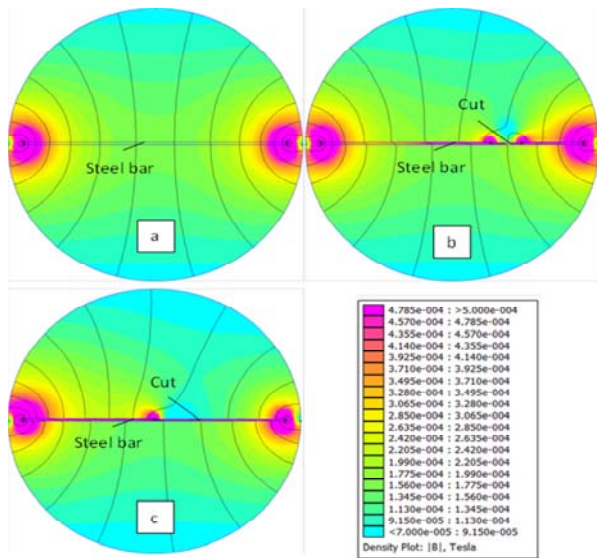


Fig. 4 Results of simulation in FEMM: a) not damaged PC bar; b) PC bar with cut of depth of 4 mm and length of 200 mm; c) PC bar with cut of depth of 4 mm and length of 850 mm.

It also worth mentioning that there is a certain effect of increase of MFL density near right angle formed by cutting, which is related with concentration of magnetic flux lines due to decrease of cross-section. That effect decreases with increase of length of cut, as one of right angle surfaces getting closer to the end of a PC bar. At the end of a PC bar there is a magnetic pole, which MFL merges with MFL from a right angle surface.

3.2 Results of the experiment

The results of the experiment are presented in Figures 5, 6 and 7. All experiments were carried out 3 times in order to gather a statistical data and avoid errors. In average standard deviation in series of 3 tests for each of the tested specimens didn't exceed, approximately, 4%. Therefore, it can be concluded that in laboratory conditions the proposed method has sufficient repeatability of results, which is important from the point of view of application for actual structures.

The results are presented in form of graphs, which vertical axis represents S parameter value; two horizontal axes represent the number of the scanned

sector. S values for scanning in forward direction correspond to the bottom horizontal axis with sector numbers from 1 to 5. The sector numbers in the horizontal bottom axis coincide with sequence numbers of sectors from the beginning of the specimen to its end, i.e. scanning in forward direction starts in sector 1 and ends in sector 5. S values for scanning in backward direction correspond to the top horizontal axis, in which sector numbers are from 5 to 1. The sector numbers in the horizontal top axis coincide with sequence numbers of sectors from the end of the specimen to its beginning, i.e. scanning in backward direction starts in sector 5 and ends in sector 1. That kind of layout of horizontal axes is selected for convenience of comparison of the results of scanning in forward and backward direction. It can be explained as follows. For example, in the case of a not damaged specimen presented in Figure 5a, scanning in forward and backward direction gives coinciding results only if values of S parameter for scanning in forward and backward direction are arranged according to their sequence number relatively to the direction of scanning (i.e., for scanning in forward direction from 1 to 5 and for scanning in backward direction – from 5 to 1). In the opposite case (i.e. if for S values for both scanning in forward and backward direction sector numbers at horizontal axis are arranged from 1 to 5), line for S values for scanning in forward direction will cross line for S values for scanning in backward direction, and, as the result, comparison between values for scanning in two directions will become less intuitive. Basically use of that arrangement of horizontal axes will allow to divide the results in two easily identifiable cases: in the first case, lines for S values for scanning in forward and backward direction coincide, which means, that a tested steel bar is not damaged; in the second case, lines for S values for scanning in forward and backward direction do not coincide, which means that a tested steel bar is damaged.

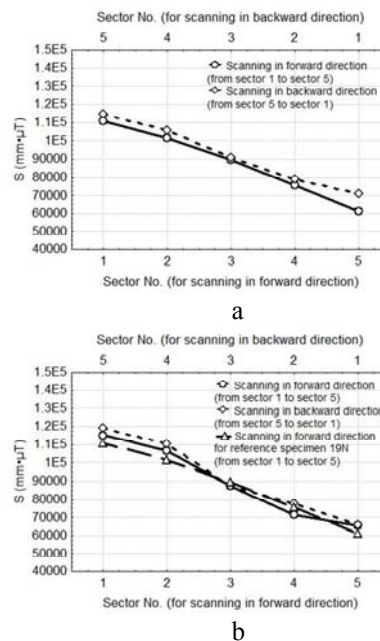
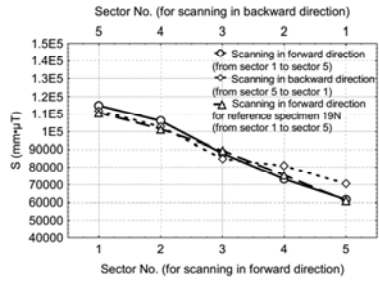


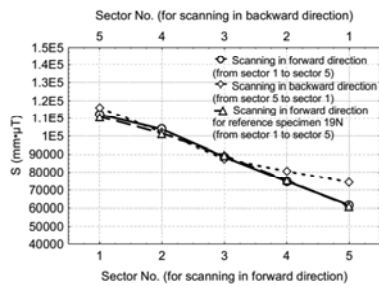
Fig. 5 Experiment results for: a) 19N; b) 19B.

In all figures values of S parameters for scanning in forward direction for reference specimen 19N are presented for convenience of comparison.

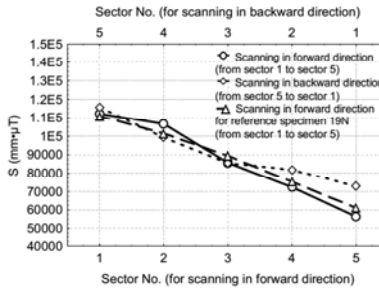
Figure 5 presents results for reference specimen 19N and specimen 19B. Comparison of Figure 5a and Figure 5b shows, that there is only a minor difference (the difference is less than standard deviation of results in series of 3 experiments) between specimen with a sheath and steel bar without sheath.



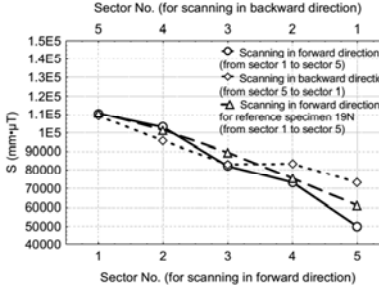
a



b



c

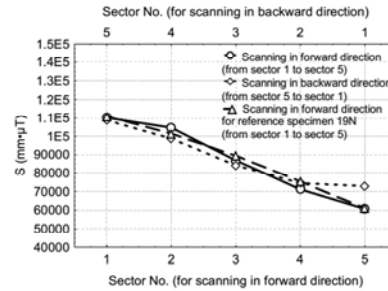


d

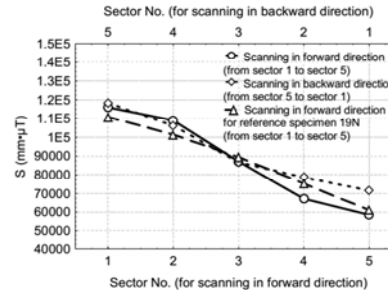
Fig. 6 Experiment results for 19L200 series: a) 19L200D1; b) 19L200D2; c) 19L200D3; d) 19L200D4.

As it can be seen from the figures, for scanning in the forward direction increase of length and depth of cuts and, therefore, weight-loss leads to visible changes of S parameter as compared to the not damaged specimen (Figure 5a). Increase of weight loss leads to

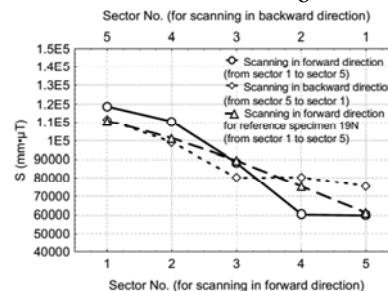
a slight increase of S value for sector 1 and 2 (sectors without damage) and more serious decrease for sectors 3-5 (sectors with damage). That is related with a redistribution of MFL density due to weight loss. The same tendency can be seen in results of the simulation in Figure 4c, where the damaged PC bar demonstrated increase MFL density for a non-damaged end and decrease of MFL density for a damaged end.



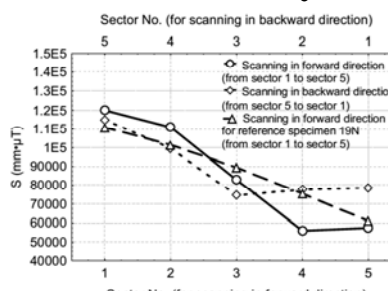
a



b



c



d

Fig. 7 Experiment results for 19L850 series: a) 19L850D1; b) 19L850D2; c) 19L850D3; d) 19L850D4.

Difference between S values for forward and backward scanning is also increasing with an increase of weight-loss. In a case of a not damaged specimen (Figure 5a), they almost coincide (especially, taking into account standard deviation of results). For specimens 19L200D1-4 and difference for scanning in

forward and backward directions is minor, because weight loss in those cases reaches, at maximum, 0.15 g/cm². In cases of specimens 19L850D1-4 difference is bigger, and weight loss reaches 0.63 g/cm².

As it can be seen from Figures 5-7 difference between values of S the sectors 4, 5 of forward scan (sectors with defects) and the sectors of 2, 1 of backward scan (undamaged sectors or sectors with lesser damage) is increasing with increase of level of damage, and in the case of the not damaged specimen (Figure 5a) there is almost no difference.

In that regard, the following points should be considered. First, in a case of scanning in forward direction sectors with weight loss will experience decrease of S parameter. Second, in a case of scanning in backward direction for the same specimen, opposite side will be not damaged and, therefore, S parameter will be larger as compared to the result for scanning in forward direction. Thus, it can be concluded that exceeding of S parameter for scanning in backward direction as compared to scanning in forward direction can be considered as an indicator of presence of defect. For example, in Figure 7d S value for scanning in forward direction for sectors 4 and 5 is significantly lower than for sectors 2 and 1 for scanning in backward direction, therefore, it can be concluded that defect is situated in sectors 4 and 5 for forward scanning, which is true. The same feature is observed for other experiment cases.

As it can be seen on all plots S (mm·μT) – Sector No., S values S values tend to decrease from sector 1 to sector 5 even in a case of not damaged specimen. It is related with a feature of the testing device, which was used during the experiment. The reason for that is somewhat unclear; presumably, it is related with a mode of operation of sensors in the scanning unit and geometry of the used specimens: range of the sensors exceed the length of the scanned sector. Therefore, while the scanning unit is approaching the end of the specimen, the range of sensors is exceeding the length of the specimen and a part of an empty space beyond the specimen is getting in a range of the sensor; as MFL density is decreasing with a decrease fo a distance to the specimen, the total MFL density of a scanned sector, in which the sensors' range catch a part of empty space beyond the specimen, is decreasing as well.

4. CONCLUSIONS

On the basis of the presented data the following conclusion can be made:

1. Change of S parameter (cumulative MFL density) is proportional to weight loss of the tested object, which allows detection of damage to PC bars.
2. Features of changes of S parameter for scanning in forward and backward direction allow to approximately identify position of detects.

In general, it can be concluded that MFL method, potentially, can be an alternative tool for detection of damage to PC bar. The method is easy to use, it is

inexpensive in operation and allows to exclude sheath influence, which complicates application of electrochemical NDT methods for PC bars. However, in the presented stage of research some tendencies and mechanism are not studied completely, and they will be investigated in further studies on the topic.

REFERENCES

- [1] Malhotra, V.M. and Carino, N.J. (Eds.), "Handbook on NDT of concrete," 2nd Edition, CRC Press, Boca Raton, 2004, pp. 243-266.
- [2] Macmaster, R.C., "Electromagnetic testing: eddy current, flux leakage, and microwave nondestructive testing," American Society for Nondestructive Testing, Materials Park, 1986, pp.608-651.
- [3] Lord, W.A., "A survey of electromagnetic methods of nondestructive testing," Plenum press, New York, 1980, pp.77-100.
- [4] Kusenberger, F.N., and Barton, J.R., "Detection of flaws in reinforcing steel in prestressed concrete," Federal Highway Administration, Washington D.C., 1981, 100 pp.
- [5] Wolf, T., and Vogel, T., "Experimental trials on the detection of reinforcement breaks with the magnetic flux leakage method," Proc. of 5th Int. Conf. on Bridge Maintenance, Safety and Management, Philadelphia, 2010, pp. 548-555.
- [6] Krause, H.J., et al., "SQUID array for magnetic inspection of prestressed concrete bridges," Physica C: superconductivity and its applications, No. 368(1-4), 2002, pp.91-95.
- [7] Maierhofer, C., Reinhardt, H., and Dobmann, G., "Non-destructive evaluation of reinforced concrete Structures. Volume 2: Non-destructive testing methods," Woodhead publishing ltd., UK, 2010, pp. 233-235.
- [8] Hirose, M., et al., "Establishment of the criterion in non-destructive test method for fracture of reinforcing steel bar by measuring magnetic flux density," Journal of Structural Engineering, Japan, No. 58A, 2012, pp. 867-878.
- [9] Sagradyan, A, et al. "Development of testing procedure for magnetic flux leakage based method of corrosion detection for reinforcement in post-tensioned concrete structures," Proceedings of Japan Concrete Institute, Vol.37, pp.1717-1722.
- [10] FEMM – Finite Element Method Magnetics. <http://femm.fostermiller.net>
- [11] Takaya, S., et al., "Influence of steel corrosion products in concrete on crack opening weight loss of corrosion," Journal of Japan Society of Civil Engineers, Ser. E2 (Materials and Concrete Structures), Japan, No. 69(2), 2013, pp. 154-165.
- [12] Cornell, R.M., and Shwertmann, U., "Iron Oxides: Structure, Properties, Occurrences and Uses," 2nd Edition, WILEY-VCH Verlag GmbH & Co. KgaA, Germany, pp. 123